JOURNAL OF MATERIALS SCIENCE: MATERIALS IN MEDICINE 7 (1996) 131–134

Effect of saline solution environment on the cyclic deformation of Ti–6Al–4V alloy

J. M. MANERO, F. J. GIL, J. A. PLANELL
Department of Materials Science and Metallurgical Engineering (ETSIIB), Universidad Politécnica de Cataluña Av. Diagonal 647, 08028-Barcelona, Spain

The present investigation studies the effect of physiological solution at 37 °C on the cyclic deformation behaviour of a Ti–6Al–4V alloy, with a microstructure corresponding to that obtained in the substrate when a sintered metallic porous coating is produced. Cyclic deformation tests have been carried out up to fracture and the fatigue crack nucleation mechanisms have been analysed. Since fatigue is a phenomenon related with plastic deformation, which is enhanced at corrosion and/or at stress concentration sites, cyclic deformation tests conducted at a level of stress above the elastic limit can provide a clear picture of the crack nucleation mechanisms involved.

1. Introduction

Titanium and titanium alloys are being increasingly used in surgical implant applications. As titanium and titanium alloys have come to substitute stainless steels and cobalt–chromium alloys in many orthopaedic prostheses, the number of revision operations due to material failure has decreased steeply [1].

Although wrought cobalt–chromium and Ti–6Al–4V alloys have a similar fatigue strength, around 550 MPa when evaluated by means of rotary bending fatigue tests [2], and a similar fatigue strength when corrosion fatigue tests are conducted in torsion, the latter has double the flexural strength of the former [3].

The elastic modulus of titanium (110 GPa), is about half that of stainless steels (200 GPa) and that of cobalt–chromium–molybdenum alloys (235 GPa) used for prosthetic implants. This is a relevant point to take into account when considering the load transfer into the bone when a joint prosthesis or an osteosynthesis device is to be designed.

Titanium is resistant to general corrosion, pitting and crevice corrosion, which may occur in other alloys as a result of the aggressive attack of body fluids [4].

When osseointegration of the implant is meant to be achieved by bone ingrowth into the pores of a sintered porous coating in a titanium alloy prosthesis, a relevant aspect which should not be neglected is the effect of sintering on the mechanical properties of the substrate alloy. The sintering process is carried out at temperatures well above the β-transus (1040 °C) of the Ti–6Al–4V alloy, and a microstructural change takes place. The final microstructure consists of an acicular alpha phase (transformed from beta phase) and a stable beta phase located between the alpha platelets [5, 6]. This microstructure yields different mechanical properties from those obtained with the "mill-annealed" microstructure obtained when the alloy is forged at 950 °C, and moreover, its behaviour under corrosion fatigue needs to be carefully considered.

2. Experimental methods and materials

The material was received as cylindrical rods of 12 mm diameter, forged at 950 °C, subsequently annealed at 700 °C for 2 h and then cooled in air.

The as-received microstructure corresponds to that known as "mill-annealed", consisting of equiaxial α-grains and β-grains which, upon cooling, transform into α-Widmanstätten plates surrounded by residual β-phase (Fig. 1).

Some specimens were held for 1 h in a tubular furnace with an argon gas atmosphere at 1050 °C, a temperature just above the β-transus for the Ti–6Al–4V alloy, and were then cooled inside the furnace at a cooling rate of 17 °C/min.

The resulting microstructure corresponds to that known as "basket weave" which consists of colonies of α-Widmanstätten plates surrounded by residual β-phase [2] (Fig. 2). This microstructure is similar to that obtained after producing a sintered metallic porous coating at the surface of the implant.

The fatigue specimens were cyclically deformed in tension–compression under strain control $R_\varepsilon = -1$, in a servohydraulic testing machine of 100 kN capacity. The strain rate was always kept constant at $6.5 \times 10^{-3}\ s^{-1}$. The total strain amplitudes investigated were $\pm 5 \times 10^{-3}$, $\pm 7 \times 10^{-3}$ and $\pm 12 \times 10^{-3}$, although only the results obtained at 7×10^{-3} were analysed. Tests were conducted in air and in a Ringer's solution environment at 37 °C. For the latter case, the specimens were deformed inside a polymethylmethacrylate container in which the solution was circulated (Fig. 3).

The nucleation of cracks at the surface, their growth inside the bulk of the specimen and the final fracture

0957–4530

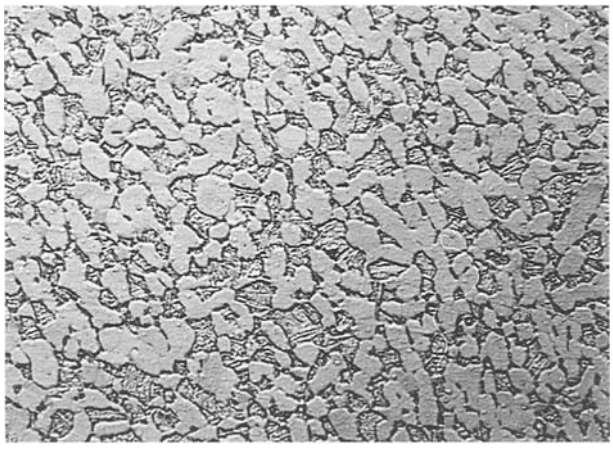

Figure 1 Mill-annealed microstructure (× 200).

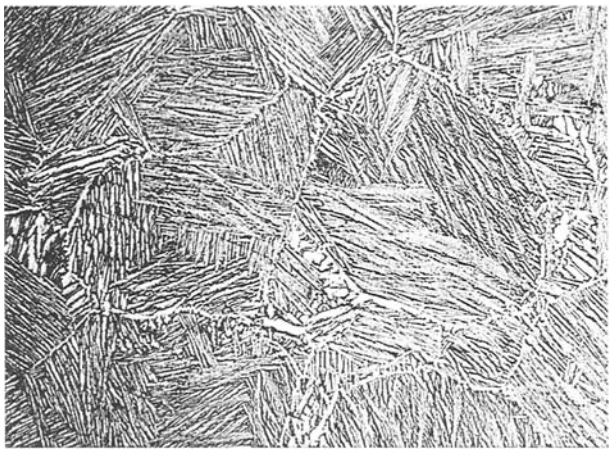

Figure 2 Basket weave microstructure (× 200).

surfaces were studied by means of scanning electron microscopy (SEM).

Finally, transmission electron microscopy (TEM) was used to study the plastic deformation mechanisms involved as well as the environmental effect on the microstructure.

3. Results and discussion

When the samples are deformed at different total strain amplitudes, the material hardens during the first two or three cycles, after which subsequent softening takes place during the whole life of the specimens, as shown in Fig. 4, for specimens deformed in air and in saline solution at 37 °C at a total strain amplitude of 7×10^{-3}. The saturation stresses are, respectively, 710 and 695 MPa. For this same total strain amplitude the fatigue life in air reaches 2700 cycles, which corresponds to a cumulative plastic strain of 3.8, while the fatigue life in Ringer's solution is only 1200 cycles or a cumulative plastic strain of 1.1. The failure in saline environment occurs always at a lower number of cycles and at lower cumulative plastic strain. When the total strain amplitude was $\pm 12 \times 10^{-3}$, the number of cycles to failure in both environments was very similar. This is due to the fact that the plastic strain is so high that the effect of corrosion is negligible.

Figure 3 Experimental device.

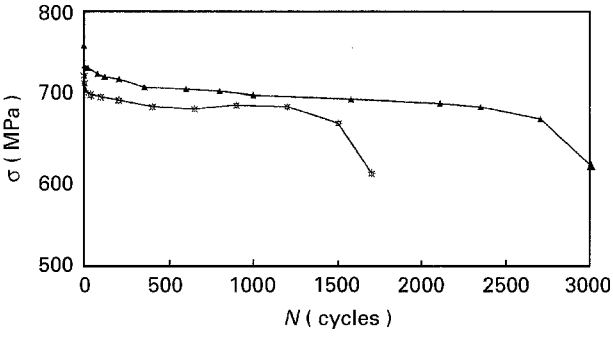

Figure 4 Cyclic softening curves: air (-▲-); Ringer's solution (-*-).

TABLE I Number of cycles to failure (N_f) and cumulative plastic strain (ε_{cum}) for the Widmanstätten microstructure

Medium	N_f	ε_{cum}
Air	2700 ± 500	3.8 ± 0.7
Saline	1200 ± 130	1.1 ± 0.1

Table I shows the number of cycles to failure (N_f) and the cumulative plastic strain (ε_{cum}) for the Widmanstätten microstructures.

For specimens tested in air, fatigue cracks seem to nucleate mainly at slip bands when plastic strains are high and at the α/β interfaces, along the α-Widmanstätten plates, when plastic strains are low (Fig. 5). However, the effect of the saline environment seems to

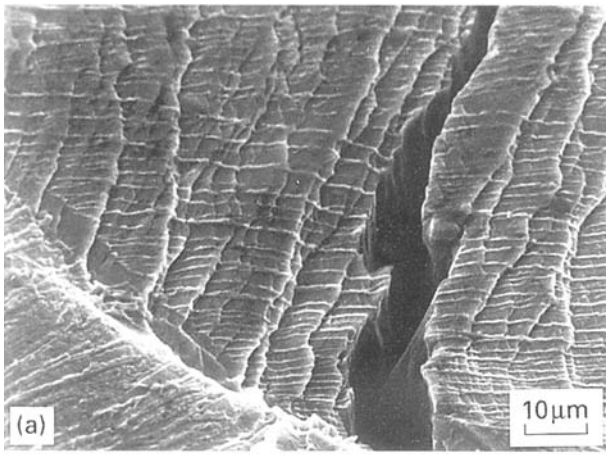

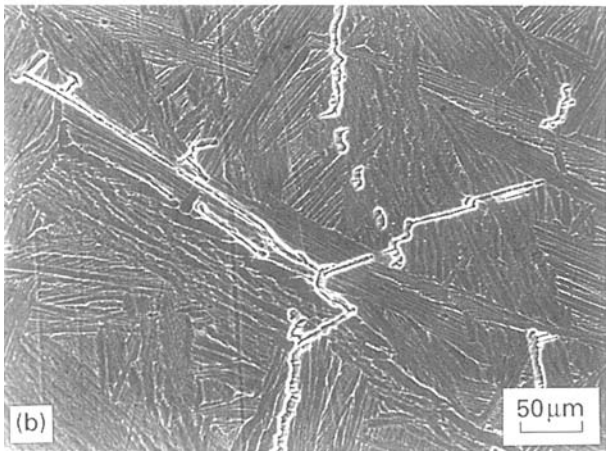

Figure 5 (a) Fatigue cracks nucleate at the slip bands when the plastic strains are high. (b) Fatigue cracks nucleate at the α/β interfaces and along α-Widmanstätten plates at low plastic strains.

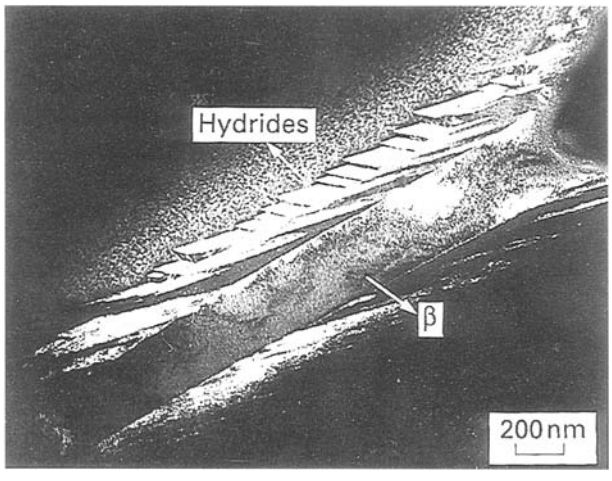

Figure 6 Dark field micrograph of the titanium hydrides.

shift the mechanism towards α/β interface nucleation for all plastic strains.

Transmission electron microscopy study of the α/β interfaces in air up to fracture shows that such interfaces accumulate a high dislocation density, which induces a phase transformation. A new face-centred cubic or face-centred tetragonal phase is formed between the α-hexagonal compact phase and the β-body-centred cubic phase (Fig. 6). Electron diffraction analysis (EDA) shows that this new phase could be a titanium hydride, TiH_x.

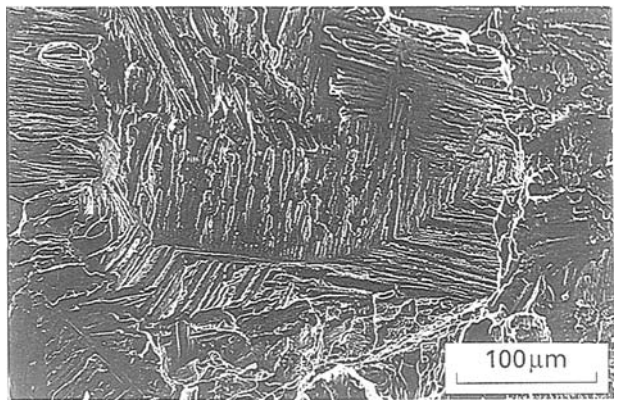

Figure 7 Fractured surface of a specimen tested in saline solution.

The formation of titanium hydride in α-Ti is associated with a volume change which is a significant activation barrier to hydride nucleation. The high density of dislocations in the α/β interfaces reduces this activation barrier inducing hydride precipitation [5, 7].

Although the amount of hydrogen in the material is low, in the region of 0.003%, it seems to be enough to produce the volume fraction of hydride phase observed by TEM. A simple calculation which takes into account the average hydride thickness on the β-plates and the average separation of such plates shows that 0.003% of interstitial hydrogen allows the formation of such a hydride. Moreover, SIMS results (secondary ionic mass spectroscopy) show that there is an absorption of hydrogen from the saline environment, since the hydrogen concentration increases by a factor of 1.5 when the hydrogen content on the microstructure of specimens tested in air and specimens tested in saline solution are compared.

It is well known that hydrides produce a severe embrittlement of Ti alloys. In fact, the fracture surface of specimens tested in air show clearly brittle propagation of the crack along the Widmanstätten plates (or α/β) interfaces [8, 9] (Fig. 7).

The effect of the saline solution environment seems to accelerate such process. Both the temperature and the diffusion of hydrogen from the aqueous solution could play significant roles. This would explain why crack nucleation always takes place at α/β interfaces and why the fatigue life is significantly decreased (Fig. 8).

It can be concluded that the high dislocation density at the α/β interfaces promotes precipitation of a titanium hydride when the microstructure of the alloy corresponds to α-Widmanstätten, which is the microstructure of the Ti–6Al–4V alloy obtained when a sintered porous coating is produced. The titanium hydride very severely embrittles the alloy and therefore the fatigue life is severely shortened. This effect is enhanced under an aqueous environment.

Since the level of loads on a Ti–6Al–4V porous coated joint prosthesis will never be so high as to produce general plastic flow, plastic deformation will only take place at certain stress concentration sites and consequently the whole process described up to fracture will take a much longer time. However, the

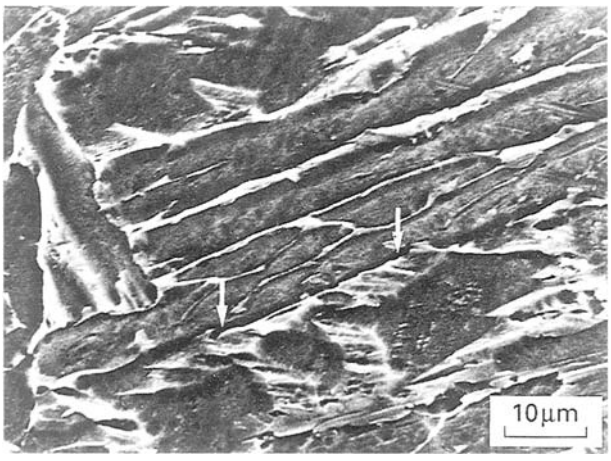

Figure 8 Specimens deformed in a Ringer's solution. Fatigue cracks nucleate at the α/β interphases.

possibility of corrosion-fatigue crack nucleation due to hydride formation at stress concentration sites should be taken into account when such an alloy microstructure is present.

References

1. B. P. BANNOM and E. E. MILD, in "Titanium alloys in surgical implants" (ASTM Special Technical Publication 796, 1983) p. 7.
2. C. B. DITTMAR, G. W. BAUER and D. EVERS, in "Titanium and titanium alloys", edited by U. Zwicker (Springer Verlag, Berlin, 1974) p. 330.
3. M. A. IMAM, A. C. FRAKER and C. M. GILMORE, "Corrosion and degradation of implant materials", ASTM STP 684 (American Society for Testing and Materials, Philadelphia, 1979) pp. 128–143.
4. R. VAN NOORT, "Review titanium: the implant material of today", *J. Mater. Sci.* (1987) 3801–3811.
5. M. J. DONACHIE, in "Titanium. A technical guide", edited by M. J. Donachie (ASM International, Ohio, 1989) p. 30.
6. S. D. COOK, N. THONGPREDA, R. C. ANDERSON and R. J. HADDAD, *J. Biomed. Mater. Res.* **22** (1988) 287–302.
7. D. BANERJEE, C. G. SHELTON, B. RALPH and J. C. WILLIAMS, *Acta Metall.* **1** (1989) 125.
8. J. M. MANERO, F. J. GIL and J. A. PLANELL, *Anales de Mecánica de la Fractura* **11** (1994) 399–404.
9. *Idem., Anales de Mecánica de la Fractura* **11** (1994) 420–426.

Received 4 May
and accepted 5 May 1995